DESY 00-103
July 2000

Geometric scaling for the total $\gamma^* p$ cross section in the low x region

A. M. Staśto[(a,b)], K. Golec-Biernat[(b,c)] and J. Kwieciński[(b)]

[(a)] *INFN, Sezione di Firenze, Largo E. Fermi 2, 50125 Firenze, Italy*[1]

[(b)] *Department of Theoretical Physics, H. Niewodniczański Institute of Nuclear Physics, ul. Radzikowskiego 152, 31-342 Kraków, Poland*[2]

[(c)] *II Institut für Theoretische Physik, Universität Hamburg, Luruper Chaussee 149, 22761 Hamburg, Germany*[3]

Abstract

We observe that the saturation model of deep inelastic scattering, which successfully describes inclusive and diffractive data at small x, predicts a geometric scaling of the total $\gamma^* p$ cross section in the region of small Bjorken variable x. The geometric scaling in this case means that the cross section is a function of only one dimensionless variable $\tau = Q^2 R_0^2(x)$, where the function $R_0(x)$ (called saturation radius) decreases with decreasing x. We show that the experimental data from HERA in the region $x < 0.01$ confirm the expectations of this scaling over a very broad region of Q^2. We suggest that the geometric scaling is more general than the saturation model.

[1]e-mail: stasto@fi.infn.it
[2]e-mail: jkwiecin@solaris.ifj.edu.pl
[3]e-mail: golec@mail.desy.de

It has recently been observed that the ep deep inelastic scattering (DIS) data at low x [1, 2] can be very economically described with the help of the saturation model [3]. In this model the QCD dipole picture of the interaction between the transversely (T) or longitudinally (L) polarized virtual photon γ^* (emitted by the incident electron) and the proton p was adopted. In this case the total $\gamma^* p$ cross sections are given by [4, 5, 6]

$$\sigma_{T,L}(x,Q^2) \;=\; \int d^2\mathbf{r} \int_0^1 dz \; |\Psi_{T,L}(r,z,Q^2)|^2 \; \hat{\sigma}(r,x)\,, \tag{1}$$

where $\Psi_{T,L}$ is the **wave function** for the splitting of the virtual photon into a $q\bar{q}$ pair (dipole), and $\hat{\sigma}$ is the imaginary part of the forward scattering amplitude of the $q\bar{q}$ dipole on the proton, called the **dipole cross section**, which describes the interaction of the dipole with the proton. In addition, $\mathbf{r}$ is the transverse separation of the quarks in the $q\bar{q}$ pair, and z is the light-cone momentum fraction of the photon carried by the quark (or antiquark). As usual, $-Q^2$ is the photon virtuality and x is the Bjorken variable. The cross section (1) has a clear physical interpretation in the proton rest frame in which the $q\bar{q}$ pair formation and a subsequent interaction with the proton are clearly separated in time.

Let us recall that the standard DIS proton structure functions are related to $\sigma_{T,L}$ by

$$F_{T,L}(x,Q^2) \;=\; \frac{Q^2}{4\pi^2\alpha_{em}}\,\sigma_{T,L}(x,Q^2)\,, \tag{2}$$

and $F_2 = F_T + F_L$. The wave function of the virtual photon is given by the following equations:

$$\begin{aligned} |\Psi_T|^2 \;&=\; \frac{3\,\alpha_{em}}{2\pi^2}\sum_f e_f^2 \left\{[z^2+(1-z)^2]\overline{Q}_f^2 K_1^2(\overline{Q}_f r)\right. \\ &\quad \left. + m_f^2\; K_0^2(\overline{Q}_f r)\right\}\,, \\ |\Psi_L|^2 \;&=\; \frac{3\,\alpha_{em}}{2\pi^2}\sum_f e_f^2 \left\{4Q^2 z^2(1-z)^2 K_0^2(\overline{Q}_f r)\right\}\,, \end{aligned} \tag{3}$$

where the sum is performed over quarks with flavour f, charge e_f and mass m_f, and

$$\overline{Q}_f^2 \;=\; z(1-z)Q^2 + m_f^2\,. \tag{4}$$

The functions $K_{0,1}$ are the Bessel–Mc Donald functions.

The main assumption of the saturation model concerns the saturation property of the dipole cross section which is incorporated in the approach of ref. [3] as below:

$$\hat{\sigma}(x,r) \;=\; \sigma_0\; g\left(\frac{r}{R_0(x)}\right)\,. \tag{5}$$

The function $R_0(x)$ with the dimension of length, called saturation radius, decreases with decreasing x, while the normalization σ_0 is independent of x. When $\hat{r} \equiv r/R_0(x) \to \infty$ the

function $g(\hat{r})$ saturates to 1, so that $\hat{\sigma}(x,r) \to \sigma_0$. In the realization [3] of the saturation model

$$g(\hat{r}) \;=\; 1 - \exp\left(-\hat{r}^2/4\right). \tag{6}$$

The fact that the dipole cross section (5) is limited by the energy independent cross section σ_0 may be regarded as a unitarity bound. This reflects the fact that the small x increase of DIS structure functions generated by pure DGLAP or linear BFKL evolution has to be tamed by unitarization effects [7]-[19].

The characteristic feature of eq. (5) is its "geometric scaling", i.e. $\hat{\sigma}(x,r)$ only depends on the dimensionless ratio $r/R_0(x)$, and its energy dependence is entirely driven by the saturation radius $R_0(x)$. The scaling property of (5) with σ_0 independent of x resembles geometric scaling of hadron-hadron scattering [20]. In the latter case the relevant quantity is the scattering amplitude in the impact parameter representation $G(b^2,s)$, where b is the impact parameter and s is the CM energy squared. The geometric scaling in this case corresponds to the assumption that

$$G(b^2,s) \to G(\beta)\,, \tag{7}$$

where $\beta = b^2/R^2(s)$ with $R(s)$ corresponding to the interaction radius which increases with increasing energy. The analogy between scaling exhibited in hadron-hadron collisions and in deep inelastic scattering should not be taken too literally. For example, the two radii have different physical interpretation, and moreover, they show completely different energy dependence since the saturation radius $R_0(x)$ decreases with increasing energy (for $x \simeq Q^2/s \to 0$).

The assumption about the scaling property of the dipole cross section (5) has profound consequences for the measured $\gamma^* p$ cross section $\sigma_{\gamma^* p} = \sigma_T + \sigma_L$. If we neglect the quark masses m_f in the photon wave functions (3) we can rescale the dipole size $r \to r/R_0(x)$ in eq. (1) such that the integration variables are dimensionless. Thus, after the integration $\sigma_{\gamma^* p}$ becomes a function of only one dimensionless variable $\tau = Q^2 R_0^2(x)$, instead of x and Q^2 separately,

$$\sigma_{\gamma * p}(x,Q^2) \;=\; \sigma_{\gamma * p}(\tau)\,, \tag{8}$$

where the scale for $\sigma_{\gamma * p}$ is provided by the dipole cross section normalization σ_0. The non-zero light quark mass does not lead to a significant breaking of the scaling (8). Let us emphasize again that the new scaling for $\sigma_{\gamma^* p}$, valid in the low x region, is obtained due to the assumption that (5) depends on r and x through the dimensionless combination $r/R_0(x)$. Following the discussion in [3] it is easy to show that with the realization (6) we smoothly change the behaviour of (8),

$$\sigma_{\gamma * p} \sim \sigma_0 \qquad \longrightarrow \qquad \sigma_{\gamma * p} \sim \sigma_0/\tau\,, \tag{9}$$

(modulo logarithmic modifications in τ) when τ changes from small to large values, respectively. The aim of this paper is to demonstrate that the DIS data do indeed approximately exhibit the geometric scaling (8) with the property (9).

Let us discuss at first the parameterization of the saturation radius $R_0(x)$. In ref. [3] the saturation radius form was postulated as follows

$$R_0(x) \,=\, \frac{1}{Q_0}\,\left(\frac{x}{x_0}\right)^{\lambda/2}\,, \tag{10}$$

where $Q_0 = 1$ GeV. The parameters $x_0,\ \lambda > 0$ together with the dipole cross section normalization σ_0 were fitted to all inclusive DIS data with $x < 0.01$. A very good description of data was obtained down to the region $Q^2 < 1$ GeV^2. The saturation model was in particular able to describe the transition from the region of DIS to the region of low values of Q^2. Also DIS diffractive data were described without additional tuning of the parameters. For a recent related analyses see [21] and also [22].

Below we show that $R_0(x)$ can also be determined differently in a less model-dependent way. To this aim let us observe that after suitable extension of the saturation model to the low Q^2 region including the photoproduction limit $Q^2 = 0$, the x dependence of the saturation radius $R_0(x)$ can be correlated with the energy dependence of the total photoproduction cross section $\sigma_{\gamma p}$. In order to extend the saturation model to the region of low Q^2 we replace, following ref. [3], x by $\bar{x}$ defined as:

$$\bar{x} = x\left(1 + \frac{4m_f^2}{Q^2}\right) \tag{11}$$

in the argument of $R_0(x)$ in eq. (5) and keep $m_f \neq 0$. The variable $\bar{x}$ is related to the total energy W by

$$\bar{x} = \frac{Q^2 + 4m_f^2}{W^2}\,. \tag{12}$$

We note that the saturation model based on eqs. (1)-(6) can now be extended down to the region $Q^2 = 0$. The photoproduction cross section is given by equations (1,3) with $Q^2 = 0$, $\bar{Q}_f^2 = m_f^2$ and with x replaced by $\bar{x} = 4m_f^2/W^2$. The dominant contribution to the photoproduction cross section comes from the integration region $1/m_f^2 \gg r^2 \gg R_0^2(x)$ in the corresponding integral on the right hand side in eq. (1). In this region we can set $m_f^2 K_1^2(m_f r) \,\simeq\, 1/r^2$ and $\hat{\sigma}(x,r) \,\simeq\, \sigma_0$. This gives the following relation between photoproduction cross section and the saturation radius

$$\sigma_{\gamma p}(W) \,=\, \bar{\sigma_0}\ln\left(\frac{1}{m_f^2\, R_0^2(\bar{x})}\right)\,. \tag{13}$$

The parameter $\bar{\sigma_0}$ is related to the overall normalization of the dipole cross section σ_0 by $\bar{\sigma_0} = (2\alpha_{em}/3\pi)\sigma_0$. From equation (13) we finally obtain the following prescription for the saturation radius

$$R_0^2(\bar{x}) = \frac{1}{m_f^2}\,\exp\left(-\frac{\sigma_{\gamma p}}{\bar{\sigma_0}}\right)\,. \tag{14}$$

For $\sigma_{\gamma p}$ we take the Donnachie–Landshoff parameterization [23]

$$\sigma_{\gamma p} \,=\, a\ \bar{x}^{-0.08}\,, \tag{15}$$

where we set $m_f = 140$ MeV (following [3]) in eqs. (12) and (14). Using results of the fit presented in [23] we find

$$a \,=\, 68\,\mu b \left(\frac{4m_f^2}{1\mathrm{GeV}^2}\right)^{0.08} \,. \tag{16}$$

For $\bar{\sigma_0}$ we set 23 μb to obtain a good description of data.

Let us now confront the implications of geometric scaling (8) with experimental data on deep inelastic scattering at low x. In Fig. 1 we show experimental data [1] on the total cross section $\sigma_{\gamma^* p}$ plotted versus scaling variable $\tau = Q^2 R_0^2(x)$, with $R_0(x)$ obtained from Eq. (14). We include all available data for $x < 0.01$ in the range of Q^2 values between 0.045 GeV^2 and 450 GeV^2.

We see that to the data exhibit geometric scaling over a very broad region of Q^2. We can also clearly see the change of shape of the dependence of $\sigma_{\gamma^* p}$ on τ from the approximate $1/\tau$ dependence at large τ to the less steep dependence at small τ. Thus the asymptotic relations (9) are also to a good approximation confirmed. The approximate asymptotic $1/\tau$ dependence reflects the fact that the cross section $\sigma_{\gamma^* p}$ scales as $1/Q^2$ (modulo logarithmic corrections) and its energy dependence is governed by $1/R_0^2(x)$. Less steep dependence corresponds to the fact that at small values of τ the total cross section grows weaker with energy than $1/R_0^2(x)$ due to saturation of the dipole cross section, see eq. (5).

We also found a symmetry between the regions of large and small τ for the function $\sqrt{\tau}\sigma_{\gamma^* p}$, which is illustrated in Fig. 2. For the asymptotic values of τ this is a manifestation of the relations (9). It is remarkable that Fig. 2 seems to indicate the presence of symmetry of $\sqrt{\tau}\sigma_{\gamma^* p}$ with respect to the transformation

$$\tau \quad \longleftrightarrow \quad 1/\tau \tag{17}$$

in the whole region of τ.

We have also tried the power law parameterization for the radius,

$$R_0^2(x) \sim x^{\lambda} \,, \tag{18}$$

where $0.3 < \lambda < 0.4$, in particular the original form proposed in [3] (see eq. (10)), and found that the data also exhibit the geometric scaling with this choice of parameterization. The approximate $1/\tau$ dependence at large τ corresponds to the $x^{-\lambda}$ behaviour of the proton structure function F_2 at large Q^2.

In the photoproduction case, the parameterization (18) combined with relation (13) would correspond to the logarithmic dependence on energy of the photoproduction cross section, i.e.

$$\sigma_{\gamma p} \sim \ln(\bar{x}) \tag{19}$$

We do therefore find that both prescriptions for $\sigma_{\gamma p}$ eq. (15) and eq. (19) give numerically similar results.

In Fig. 3 we show contours corresponding to different values of variable τ in (x, Q^2) plane together with experimental points for these values of τ. Geometric scaling means that $\sigma_{\gamma^* p}$ is constant along each line. To be precise for each value of τ we plot experimental points within the bin $(\ln(\tau) \pm \delta)$ with $\delta = 0.1$. We see from this figure that for each τ there are several experimental points for which x varies as much as two orders of magnitude and Q^2 changes by a factor of 4. Despite of that, all points along each line in Fig. 3 are transformed to a narrow spread of points for a particular value of τ in Figs. 1 and 2, thus exhibiting geometric scaling.

In order to show that the geometric scaling is confined only to the small x region we show a similar plot as in Fig. 1, but for the experimental data with $x > 0.01$ [1, 2]. It is evident that the geometric scaling is significantly violated in the region of large x, see Fig. 4.

We would like to emphasize that the (approximate) geometric scaling should predominantly be regarded as a remarkable regularity of DIS experimental data at low x.

Although this scaling has been inspired by the saturation model of ref. [3], its significance goes presumably far beyond this model. In its essence the new scaling is a manifestation of the presence of an internal scale (saturation scale) characterizing dense partonic systems, $Q_s(x) \sim 1/R_0(x)$. This scale emerges from a pioneering work of [7], which was subsequently analyzed and generalized in [8]- [19]. In the analysis [11], and more recently in [18], the scaling properties similar to those postulated in (5) were found. An independent formulation [12] of the small x processes, gives the same overall picture with the saturation scale. At a deeper level, the geometric scaling for small-x processes may reflect self similarity or conformal symmetry of the underlying dynamics. More detailed studies are under way, see [16]-[19].

To sum up we have shown that the experimental data on deep inelastic ep scattering at low x exhibit geometric scaling, i.e. the total cross section $\sigma_{\gamma^* p}(x, Q^2)$ is the function of only one dimensionless variable $\tau = Q^2 R_0^2(x)$. This regularity was found to hold over the very broad range of Q^2 from 0.045 GeV^2 to 450 GeV^2. It would be interesting to understand in detail a possible dynamical origin of this simple regularity.

Acknowledgments

We thank Jochen Bartels and Genya Levin for useful comments and Larry McLerran for useful correspondance. This research has been partially supported by the EU Framework TMR programme, contract FMRX-CT98-0194, Deutsche Forschungsgemeinschaft and the Polish Commitee for Scientific Research grants Nos. KBN 2P03B 120 19, 2P03B 051 19.

References

[1] H1 Collaboration (S. Aid et al.), *Nucl. Phys.* **B 470** (1996) 3; ZEUS Collaboration (M. Derrick et al.), *Z. Phys.* **C 72** (1996) 399; H1 Collaboration (C. Adloff et al.), *Nucl. Phys.* **B 497** (1997) 3; ZEUS Collaboration (J. Breitweg et al.), *Phys. Lett.* **B 407** (1997) 432; ZEUS Collaboration (J. Breitweg et al.), DESY-00-071, `hep-ex/0005018`.

[2] BCDMS collaboration (A.C. Benvenuti et al.), *Phys. Lett.* **B 223** (1989) 485; NMC collaboration (M. Arneodo et al.), *Phys. Lett.* **B 364** (1995) 107; E665 collaboration (M.R. Adams et al.), *Phys. Rev.* **D 54** (1996) 3006; SLAC collaboration, *Phys. Lett.* **B 282** (1992) 475; EMC collaboration (Aubert et al.), *Nucl. Phys.* **B 259** (1985) 189.

[3] K. Golec-Biernat and M. Wüsthoff, *Phys. Rev.* **D59** (1999) 014017; *Phys. Rev.* **D60** (1999) 114023.

[4] J.D. Bjorken, J.B. Kogut and D.E. Sopper, *Phys. Rev.* **D3** (1971) 1382.

[5] N.N. Nikolaev and B.G. Zakharov, *Z. Phys.* **C49** (1991) 607; *Z. Phys* **C53** (1992) 331; *Z. Phys.* **C64** (1994) 651; *JETP* **78** (1994) 598.

[6] A. H. Mueller, *Nucl. Phys.* **B415** (1994) 373; A. H. Mueller and B. Patel, *Nucl. Phys.* **B425** (1994) 471; A. H. Mueller, *Nucl. Phys.* **B437** (1995) 107.

[7] L.V. Gribov, E.M. Levin and M.G. Ryskin, *Phys. Rep.* **100** (1983) 1.

[8] A.H. Mueller and Jian-wei Qiu, *Nucl. Phys.* **B268** (1986) 427 ; A.H. Mueller, *Nucl. Phys.* **B335** (1990) 115; Yu.A. Kovchegov, A.H. Mueller and S. Wallon, *Nucl. Phys.* **B507** (1997) 367. A.H. Mueller, *Eur. Phys. J.* **A1** (1998) 19; *Nucl.Phys.* **A654** (1999) 37c; *Nucl.Phys.* **B558** (1999) 285.

[9] J. C. Collins and J. Kwieciński, *Nucl. Phys.* **B335** (1990) 89.

[10] J. Bartels, G.A. Schuler and J. Blümlein, *Z. Phys.* **C50** (1991) 91; *Nucl. Phys. Proc. Suppl.* **18 C** (1991) 147; J. Bartels, *Phys. Lett.* **B298** (1993) 204; *Z. Phys.* **C60** (1993) 471; *Z. Phys.* **C62** (1994) 425; J. Bartels and M. Wüsthoff, *Z. Phys.* **C66** (1995) 157; J. Bartels and C. Ewerz, *JHEP* **9909** (1999) 026.

[11] J. Bartels and G. Levin, *Nucl. Phys.* **B387** (1992) 617.

[12] L. McLerran and R. Venugopalan, *Phys. Rev.* **D49** (1994) 2233, *Phys. Rev.* **D49** (1994) 3352, *Phys. Rev.* **D50** (1994) 2225; A. Kovner, L. McLerran and H. Weigert, *Phys.Rev.* **D52** (1995) 6231, *Phys. Rev.* **D52** (1995) 3809; R. Venugopalan, *Acta. Phys. Polon.* **B30** (1999) 3731.

[13] A. Białas and R. Peschanski, *Phys. Lett.* **B355** (1995) 301; *Phys. Lett.* **B378** (1996) 302; *Phys. Lett.* **B387** (1996) 405; A. Bialas *Acta Phys. Polon.* **B28** (1997) 1239; A. Bialas and W. Czyz, *Acta Phys.Polon.* **B29** (1998) 2095; A. Białas, H. Navelet and R. Peschanski, *Phys. Rev.* **D57** (1998) 6585; *Phys. Lett.* B427 (1998) 147; `hep-ph/0009248`.

[14] G.P. Salam, *Nucl. Phys.* **B449** (1995) 589; *Nucl. Phys.* **B461** (1996) 512; *Comput. Phys. Commun.* **105** (1997) 62; A.H. Mueller and G.P. Salam, *Nucl. Phys.* **B475** (1996) 293.

[15] E. Gotsman, E. M. Levin and U. Maor, *Nucl. Phys.* **B464** (1996) 251; *Nucl. Phys.* **B493** (1997) 354; *Phys. Lett.* **B245** (1998) 369; *Eur. Phys. J.* **C5** (1998) 303; E. Gotsman, E. M. Levin, U. Maor and E. Naftali, *Nucl. Phys.* **B539** (1999) 535; A. L. Ayala Filho, M. B. Gay Ducati and E. M. Levin, *Eur. Phys. J.* **C8** (1999) 115; E. Levin and U. Maor, `hep-ph/0009217`.

[16] Ia. Balitsky, *Nucl.Phys.* **B463** (1996) 99.

[17] J. Jalilian-Marian, A. Kovner, L. McLerran and H. Weigert, *Phys. Rev.* **D55** (1997) 5414; J. Jalilian-Marian, A. Kovner and H. Weigert, *Phys. Rev.* **D59** (1999) 014014; *Phys. Rev.* **D59** (1999) 014015; *Phys. Rev.* D59 (1999) 034007; Erratum-ibid. D59 (1999) 099903; A. Kovner, J.Guilherme Milhano and H. Weigert, OUTP-00-10P,NORDITA-2000-14-HE, `hep-ph/0004014`; H. Weigert, NORDITA-2000-34-HE, `hep-ph/0004044`.

[18] Y.V. Kovchegov, *Phys. Rev.* **D60** (1999) 034008; *Phys. Rev.* **D61** (2000) 074018; G. Levin and K. Tuchin, *Nucl. Phys.* **B537** (2000) 833; M.A. Braun, *Eur. Phys. J.* **C16** (2000) 337.

[19] Y.V. Kovchegov and L. McLerran, *Phys. Rev.* **D60** (1999) 054025; Erratum-ibid. **D62** (2000) 019901; Y.V. Kovchegov and G. Levin, *Nucl. Phys.* **B577** (2000) 221;

[20] J. Dias de Deus, *Nucl. Phys.* **B 59** (1973) 231; A. J. Buras, J. Dias de Deus, *Nucl. Phys.* **B 71** (1974) 481; J. Dias de Deus, P. Kroll, *J. Phys.* **G 9** (1983) L81; J. Dias de Deus, *Acta Phys. Polon.* **B 6** (1975) 613.

[21] W. Buchmüller, T. Gehrmann and A. Hebecker *Nucl. Phys.* **B537** (1999) 477; G. R. Forshaw, G. Kerley and G. Shaw, *Phys. Rev* **D60** (1999) 074012, *Nucl. Phys.* **A675** (2000) 80; E. Gotsman, E. Levin, U. Maor and E. Naftali, *Eur. Phys. J.* **C10** (1999) 689; M. McDermott, L. Frankfurt, V. Guzey and M. Strikman, *Eur. Phys. J.* **C16** (2000) 641; T. G. Cvetic, D. Schildknecht and A. Shoshi, *Acta Phys. Polon.* **B 30** (1999) 3265; A. Capella, E. G. Ferreiro, A. B. Kaidalov and C. A. Salgado, `hep-ph/0006233`.

[22] A. Donnachie and P.V. Landshoff, *Phys. Lett.* **B437** (1998) 408.

[23] A. Donnachie and P.V. Landshoff, *Phys. Lett.* **B296** (1992) 227.

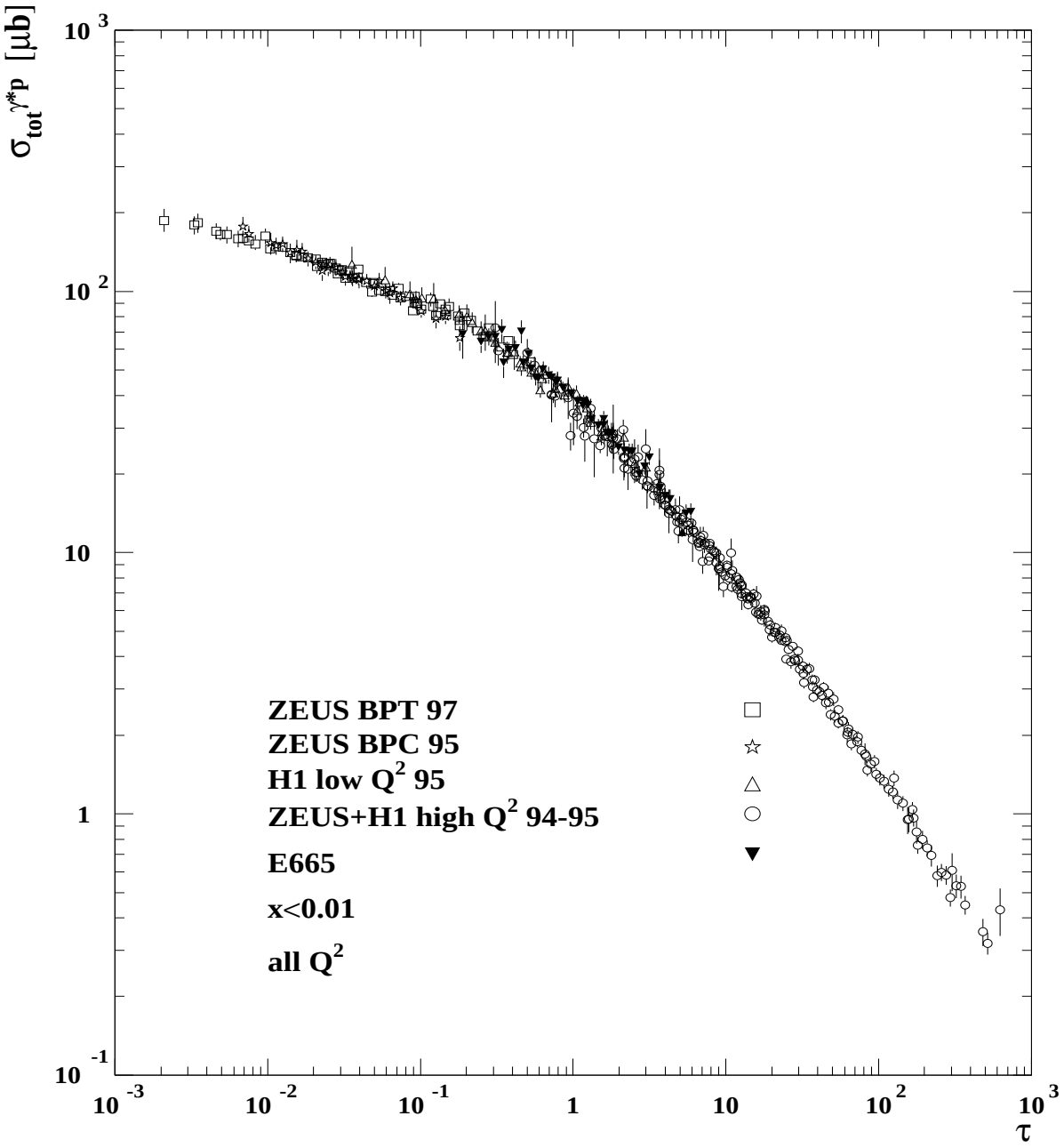

Figure 1: Experimental data on $\sigma_{\gamma^* p}$ from the region $x < 0.01$ plotted versus the scaling variable $\tau = Q^2 R_0^2(x)$.

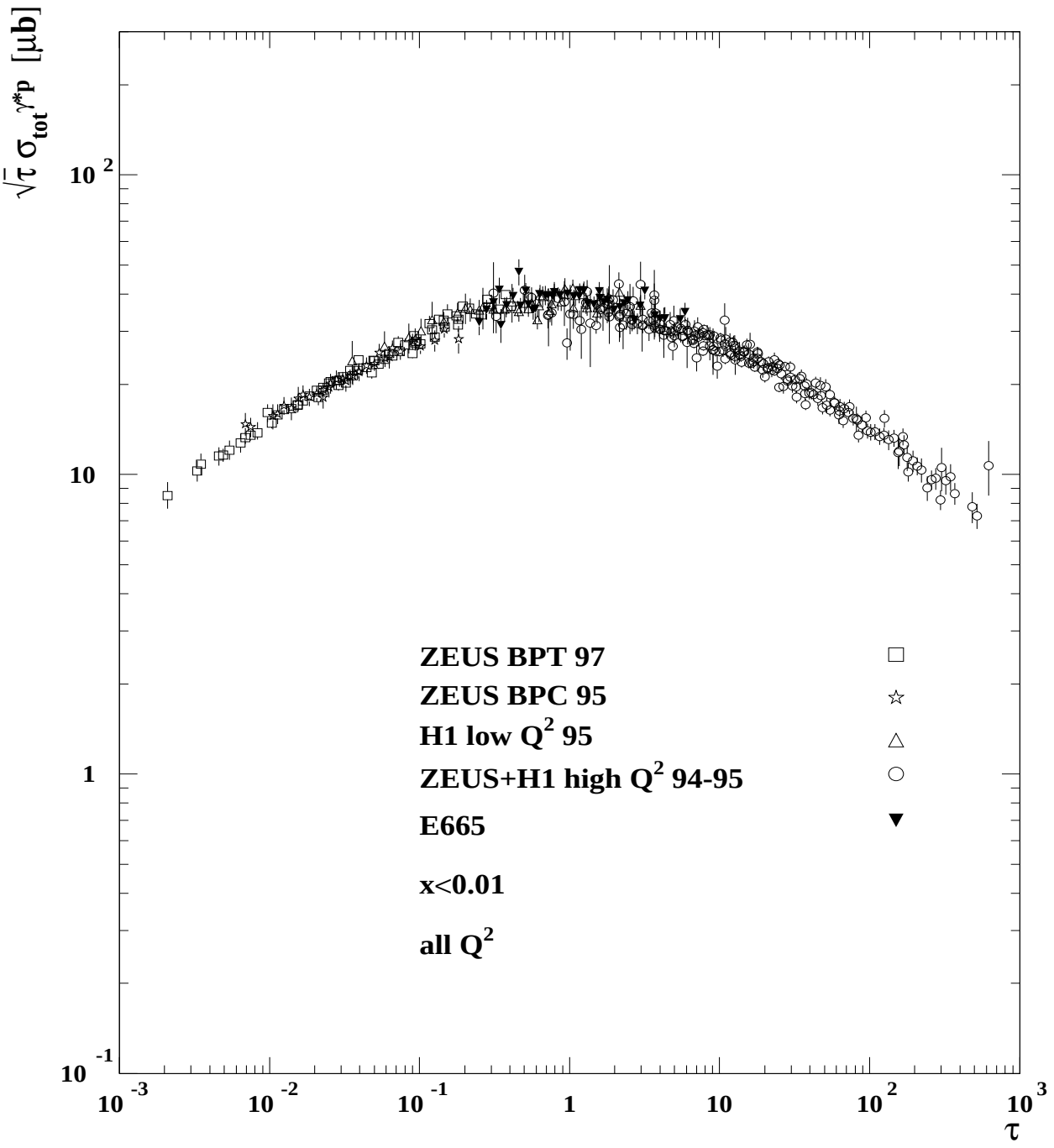

Figure 2: $\sqrt{\tau}\sigma_{\gamma^* p}$ plotted versus the scaling variable τ

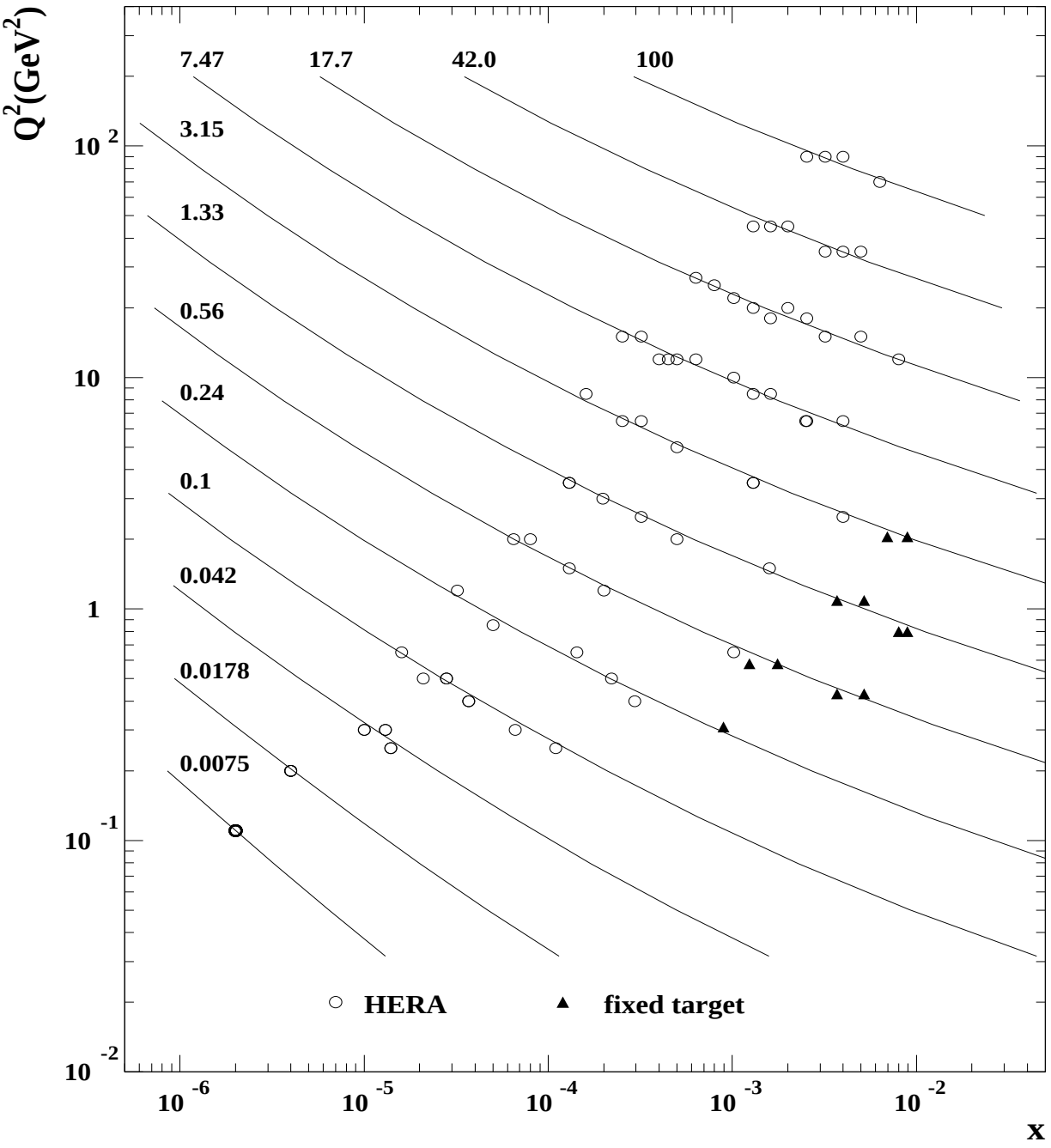

Figure 3: The lines corresponding to different values of scaling variable τ (continues curves) in the (x, Q^2)-plane. The points correspond to available experimental data located within the bins $\ln(\tau) \pm \delta$ ($\delta = 0.1$) for each value of τ. The numbers correspond to the value of τ for each curve.

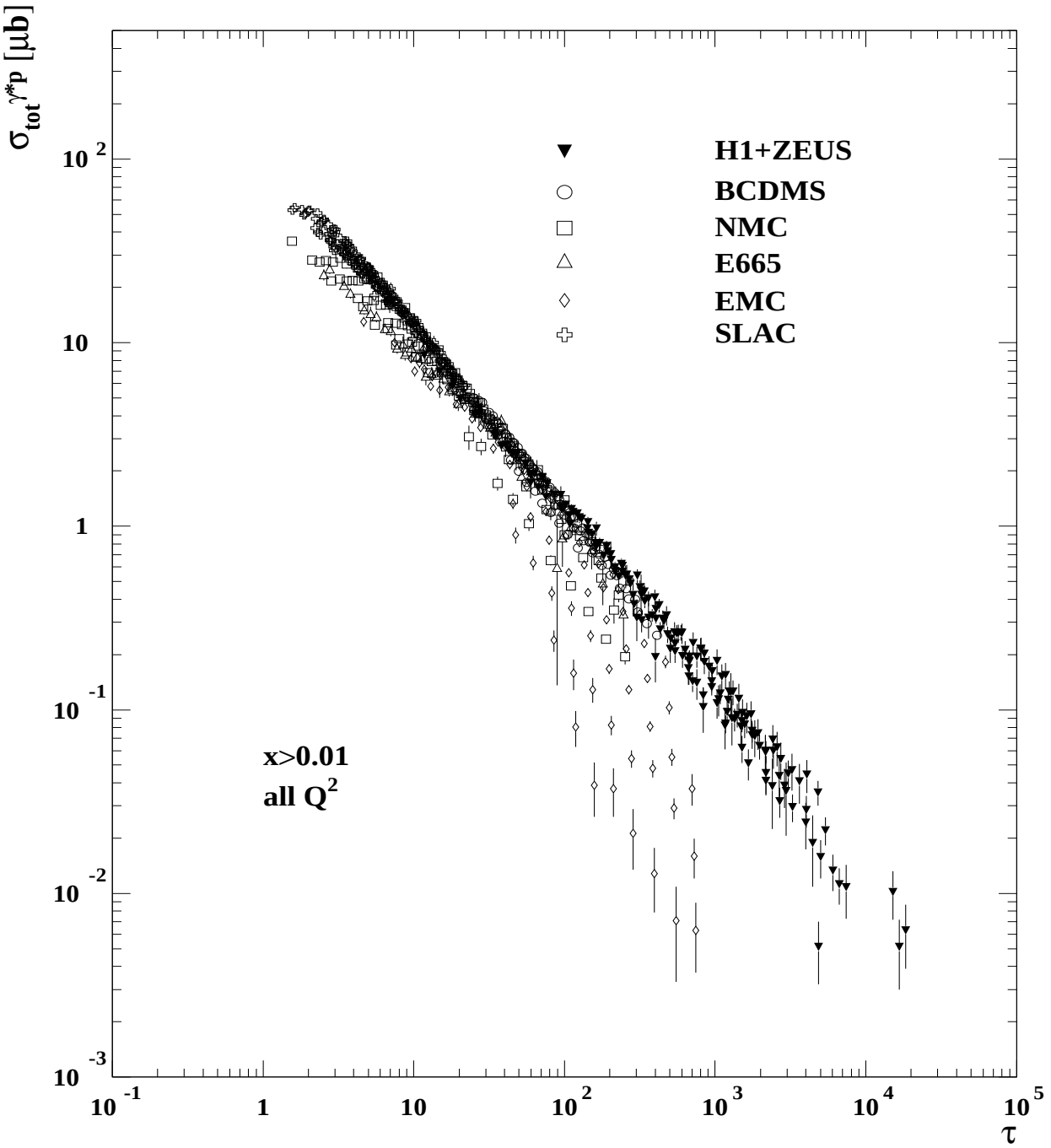

Figure 4: Experimental data on $\sigma_{\gamma^* p}$ from the region $x > 0.01$ plotted versus the scaling variable $\tau = Q^2 R_0^2(x)$.